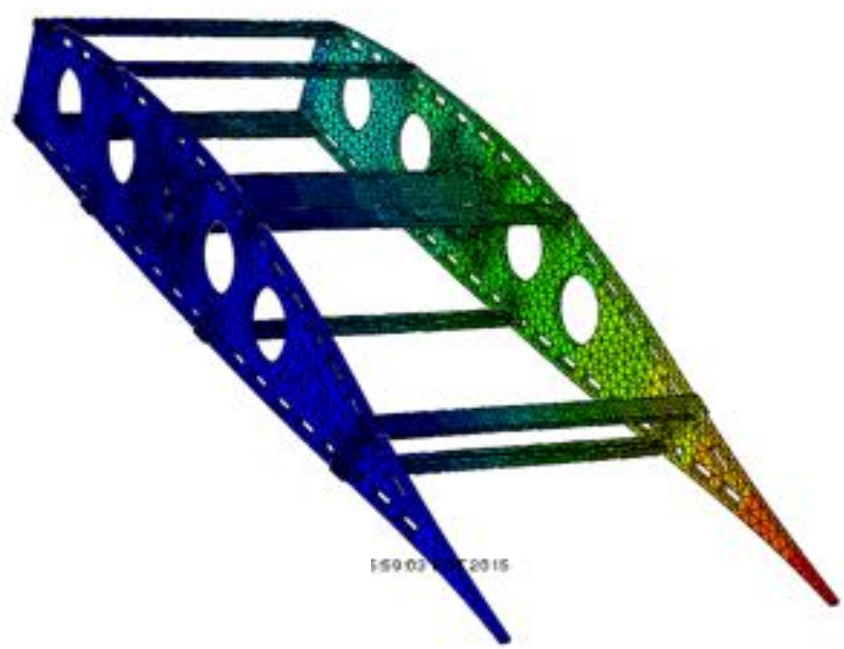

ME 461:
Finite Element
Analysis

Fall 2015

A Semester Report on:

The Development and Analysis of Airfoil Supports

Group Members:

Young Charlie, Tindall Kyle, Schweikert James, Sinisi Zach, Warner Dave

PennState
College of Engineering

Department of Mechanical and Nuclear Engineering, University Park, PA

Table of Contents

Executive Summary

The purpose of the following analysis concerning airfoil supports was conducted to ensure safe operation during testing of the airfoil itself. A section of this airfoil has been modeled using Creo Parametric, which was then converted into Abaqus to perform a Finite Element Analysis of the airfoil portion. This section of the airfoil will be tested under normal operating conditions of 300 mph. The Finite Element Analysis results will then be used to determine if the supports will be safe to operate at the given conditions.

Acknowledgements

We would like to thank Guidedwave for providing the CAD files and allowing us to use them for our report. We would also like to thank Dr. Reuben Kraft for his support and guidance throughout the semester while we worked on this project report.

List of Figures

Section 1: Background and Project Plan

The idea to analyze the stess and strain of a section of an airfoil originated from a project that was taking place at one of our groupmember's internship. This portion of the project was concerened about whether or not the airfoil would be safe when placed into a wind tunnel and tested at normal operating conditions of 300 mph. Instead of analyzing the airfoil as if it were a small isolated section in a wind tunnel, we decided to analyze the airfoil section as if it were still attached to the entire airfoil assembly.

In our analysis we will be determining how the stress is distributed through all of the support members in the airfoil section. Also another design consideration for the support members is the factor of safety associated for each, which will also be determined through the following analysis. Lastly the resulting displacements will be observed to determine if this would be a design issue.

Section 2: Development and Description of the CAD Geometry

The CAD geometry already existed for the airfoil, and was provided by Guidedwave for our use. The original design of this CAD model was for confidential purposes, therefore certain geometries have been altered to keep this confidentiality. In the original CAD model the entire airfoil was used to produce the section of the airfoil that was analyzed in this report. The original file contained a vast amount of parts and sub-assemblies, which were converted into step files. Problems arrived here when importing the files to Abaqus. This was another reason that the original CAD file needed to be altered and simplified. To do this, all screws and fasteners were removed because they would have caused a greater amount of computing time and were not the primary focus of the analysis. The skin of the airfoil was not considered in the analysis since it does not provide substantial support and our analysis is primarily concerned with the support structure within the airfoil section. Another subassembly that was not considered in the analysis was the leading edge of the airfoil section. This is because the majority of the confidential information was contained in the leading edge, and for that reason the entire subassembly was removed from the analysis.

To make the changes and alterations mentioned, the original CAD file containing all of the complexities was re-saved under a different file name. This was done so changes made did not alter the original CAD file provided by Guidedwave. From this newly saved document, alterations were maded to reduce the complexity of the file. Once the complexity was reduced a step file was created that could be imported into abaqus.

When importing the file into Abaqus a choice had to be made on whether or not to import as one solid part or as individual parts. The second option was chosen because during the first attempts of meshing, the entire solid part caused errors concerning incorrect geometry. Also, with importing each part invidually and then reassembling, a more realistic analysis was conducted because the airfoil section is composed of multiple subsequent parts instead of one individual part. The final reassembled CAD geometry can be seen in Figure 1, and the engineering print containing critical dimensions in English units can be seen in Appendix 1.

Figure 1: Assembled CAD Geometry

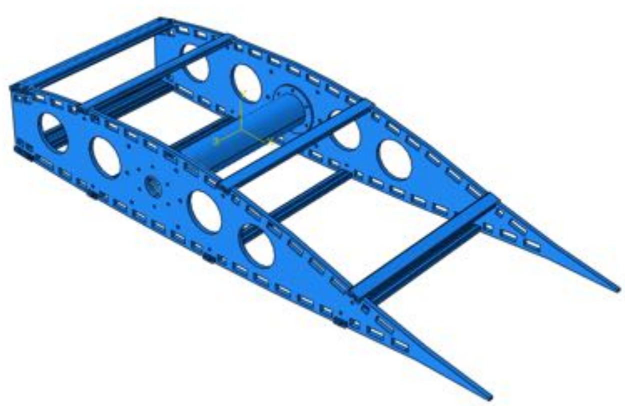

Section 3: Development of Finite Element Meshes

The next step in the analysis of the airfoil section was to create the mesh for the assembly. As mentioned earlier when trying to mesh the entire assembly at once, geometric errors were encountered and for that reason each part was meshed individually using the same meshing technique and then assembled into the final assembly.

When creating the mesh for each part we decided to use tetrahedral elements to ensure a more accurate result in our analysis. Besides the larger parts, a global mesh size of 0.01 was used for each part. This mesh size seemed to generate meshes for each part without much distortion of any elements that would yield an inaccurate result. As for the larger parts like the end panels a larger global mesh size was used to reduce the computing time when the job was submitted. It should also be noted that our analysis is not concerened with the side panels so a less accurate result is sufficient for the side panels. Figures 2 through 9 portray examples of the individual parts meshed and Figure 10 shows the final meshed assembly that was used for the analysis.

Figure 2: Meshed Mount Tube

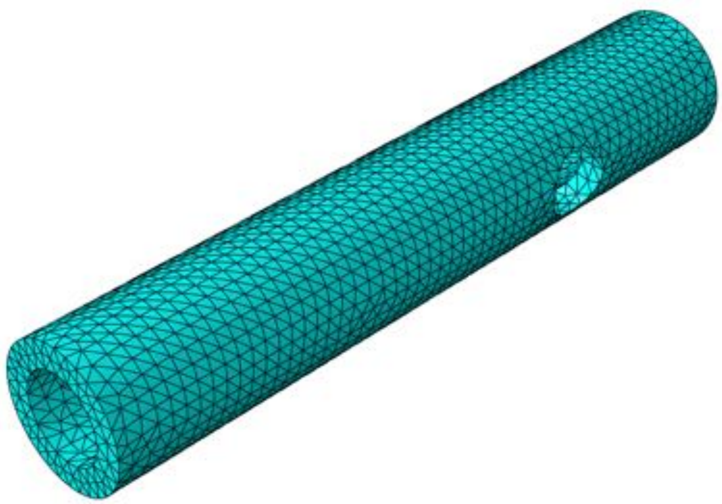

Figure 3: Stress Concentration in the Support Tube

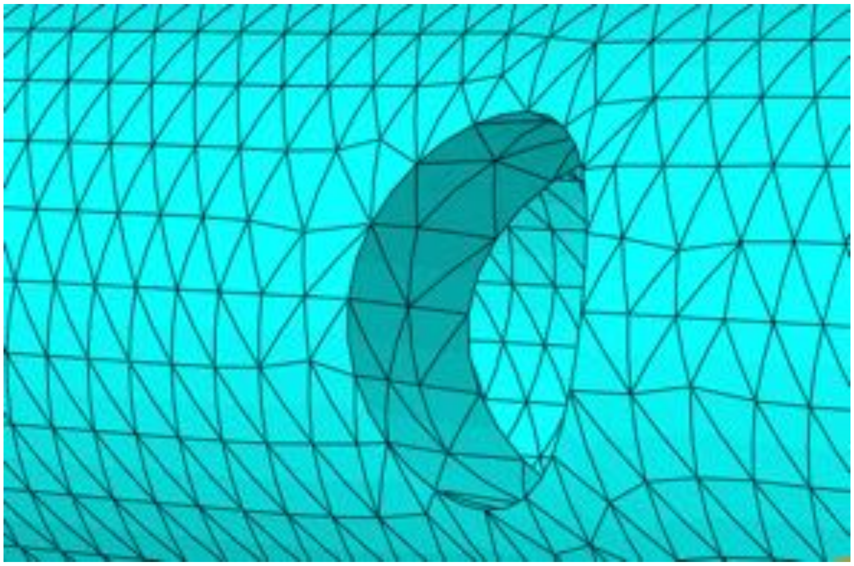

Figure 4: 10-016 Meshed Strut

Figure 5: 10-016 Meshed Side View

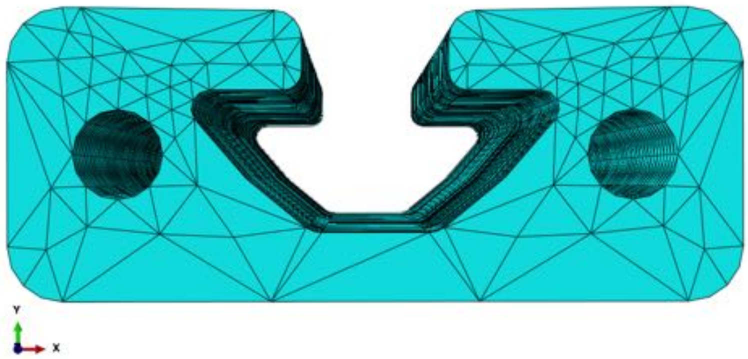

Figure 6: 10-081 Meshed Strut

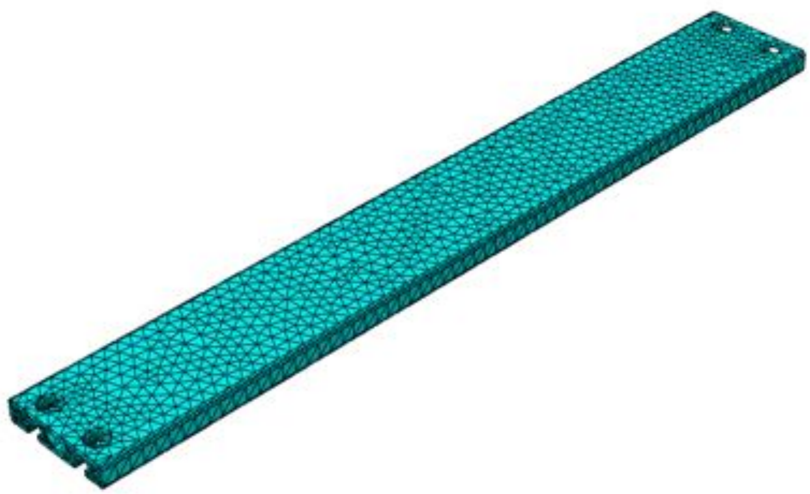

Figure 7: 10-081 Side View

Figure 8: Meshed Mount Tube Ring

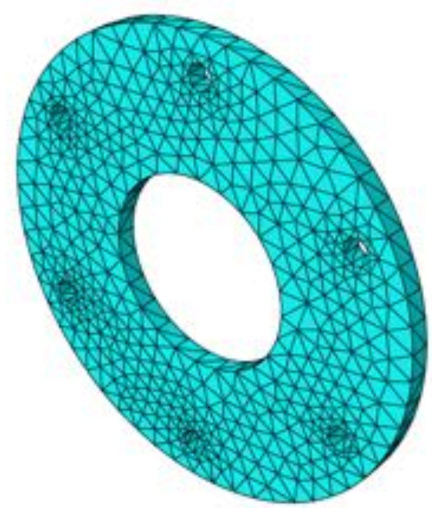

Figure 9: Meshed Side Panel

Figure 10: Final Meshed Assembly

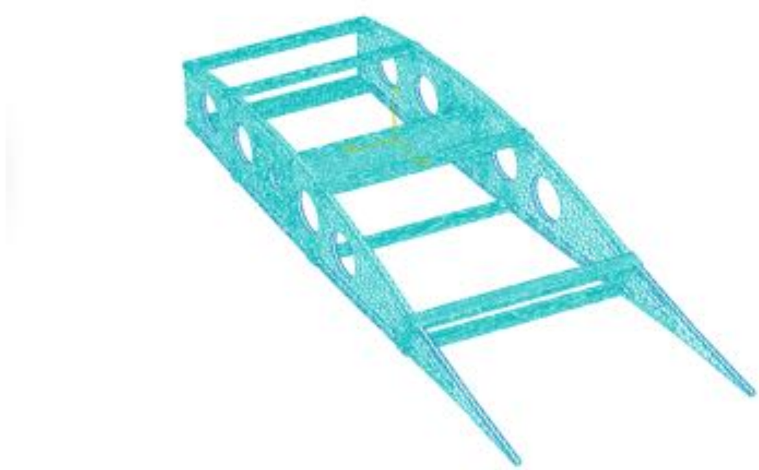

Section 4: Development and Description of the Model Assembly and Boundary Conditions

Assigning material properties and boundary conditions to the assembly was the next step in our analysis of the airfoil section. The airfoil that Guidedwave has contains a variety of materials, but the supports are primarily aluminum. Typical airfoils contain much lighterweight materials such as carbon fiber which are very stong as well, but for the project being conducted by Guidedwave the supports and panels are made of 6061-T6 Aluminum. Table 1 shows the important material properties of the aluminum alloy.

Establishing boundary conditions for the section of the airfoil was a relatively simple task. We decided to use independent part instances when assembling so that if we needed to change a mesh of a certain part we would be able to without altering the meshes of any subsequent instances. Since we are only analyzing a section of the airfoil, we can assume we are analyzing a section that is located close to the fuselage of the aircraft. Assuming this we can assume that one side of the airfoil section is rigid compared to the other. Knowing this we decided to constrain all motion of one of the side panels of the airfoil section, while loading the other side panel. The boundary conditions are represented in Figure 11.

Table 1: Material Properties of 6061-T6 Aluminum

Yield Strength (MPa)	Youngs Modulus (GPa)	Poissons Ratio	Density (kg/m^3)
310	68.9	0.33	2700

Figure 11: Boundary Conditions and Loading

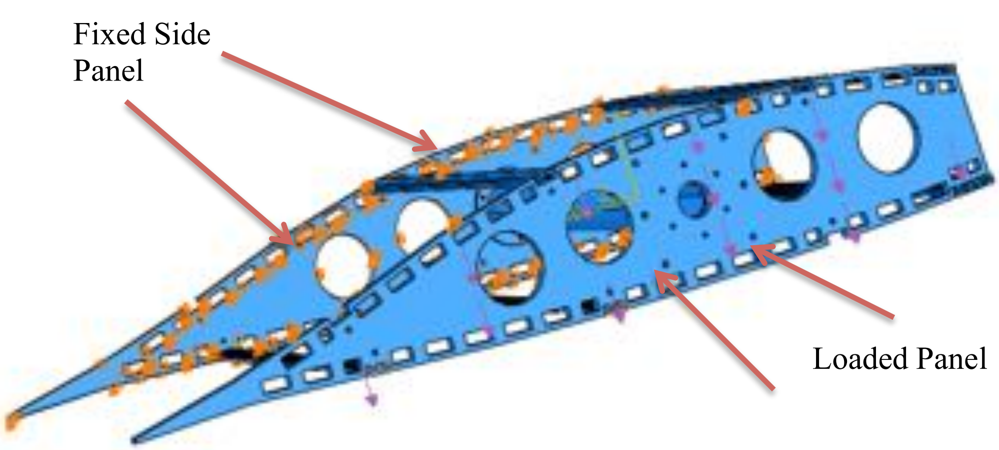

Section 5: Development and Description of Model Interactions

When a model is assembled in Abaqus, constraints or model interactions need to be identified. Without these defined model interactions, an accurate finite element analysis cannot be obtained. In the model, the development of these interactions was rather repetitive, yet straightforward to define. It should be noted that although each individual part of the assembly is constrained to another active part, the model is treated as one whole entity when fully defined. As each individual part was assembled, the mating surfaces between parts were defined as tied constraints. These tied interactions defined a condition, which under loading would keep surfaces from separating. The tied interactions are representative of a bolted, welded or bonded joint.

Prior to using tied constraints, a method of merging the individual instances with one another was attempted. This approach was found to be unsuccessful because it continuously altered the geometry of the model. For this reason, the tie constraint method was utilized. These tie constraints also resemble the bolts that were utilized in the model used by Guidedwave.

There is an issue that occurs when using tie constraints, which is the accuracy of the results. From prior sample experiments it was found that the results converge on a final value if the mesh size is small enough. However if the mesh size is too small the job submission will take much longer to run. Knowing this we were able to reduce the mesh size at critical tie contstaint locations to ensure accurate results.

Section 6: Analysis of Finite Element Model

The loading of the airfoil section was done in a single static step in which the loaded side panel was loaded with an 8000 N/m^2 surface traction. Even though this was a simple loading case the submitted job took approximately thirty minutes to execute. This execution time is not too long but if the mesh size were reduced further we would anticipate that the execution time would increase substationally. The 8000 N/m^2 surface traction was determined by a third party software used by Guided wave and was found using the pitch angle of the airfoil along with the velocity among other factors.

The simulation loading condition showed interesting reactions between the individual pieces of the airfoil. The images below indicate that with a single downward loading case a torsional load is developed. This torsion is viewable through a top plane orientation. As the airfoil is loaded, the structure reacts and twists slightly due to its geometrical design. The images below are exaggerated greatly, which is a feature in Abaqus that can be edited. The exaggerated motion gives the user a clearer representation of the reaction of flexure in the assembly being analyzed. The comparison between the loaded and unloaded assembly displacement can be seen in Figures 12 and 13.

Figure 12: (Left) Top View Unloaded, (Right) Back View Unloaded

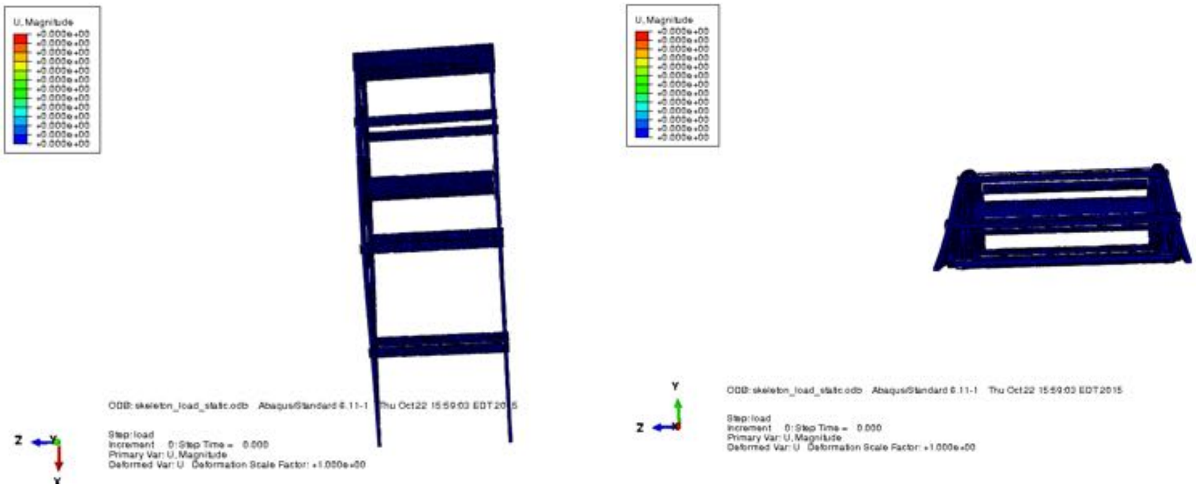

Figure 13 (Left) Deformend Top View, (Right) Deformend Back View

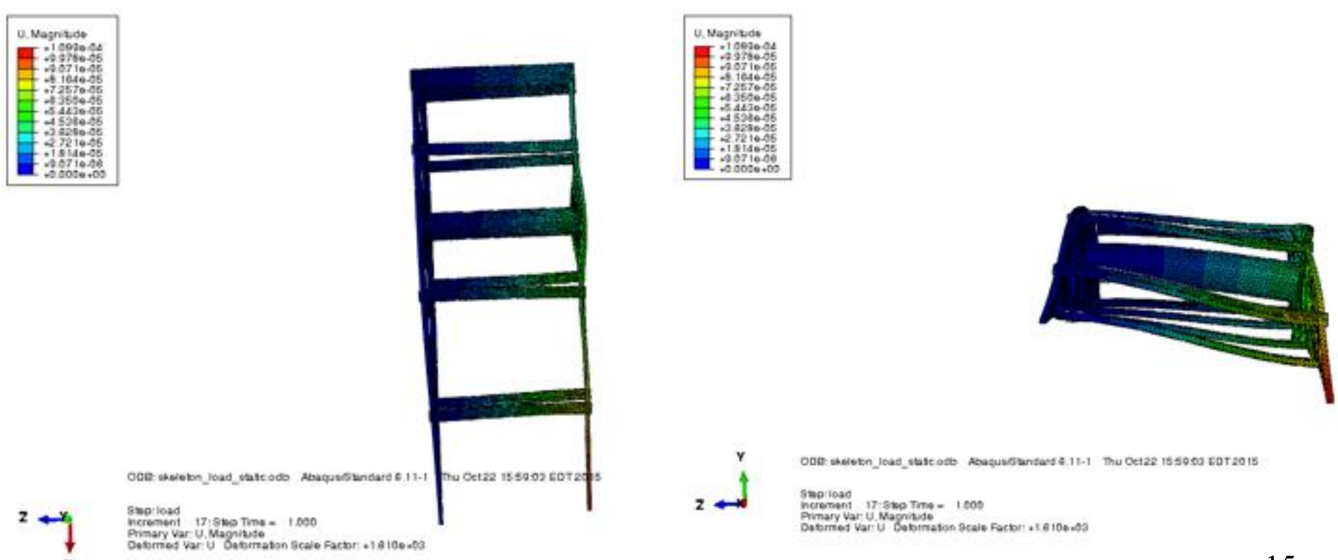

Section 7: Summary of Major Findings

The results obtained from the static load test gave interesting results. The first thing that needs to be noted is that the tied constraint was a good approach to assembling the model and applying interactions. Comparing the results obtained from abaqus to hand calculations; there was very little difference in value, which means the tied constraint worked how it should. Figure 14 shows the Von Mises stress distribution through the airfoil supports while Figure 15 shows how the airfoil section displaced in the vertical direction during loading. Figure 14 shows that the highest stress occurred primarily in the Mounting Tube, particularly at the fixed end. This makes sense since the tube is loaded as a cantilever beam and the highest stresses occur at the fixed end. It is interesting to note that the highest stresses did not occur in any of the thinner 10-6061 supports or at the location of the stress concentration. The largest Von Mises stress value was 30.39 MPa and was located at one of the tie constraints. However the majority of the stress was carried through the Mount Tube. To determine if the airfoil is safe, the results of the Mount Tube are the most significant.

Figure 14 Von Mises Stress Distribution

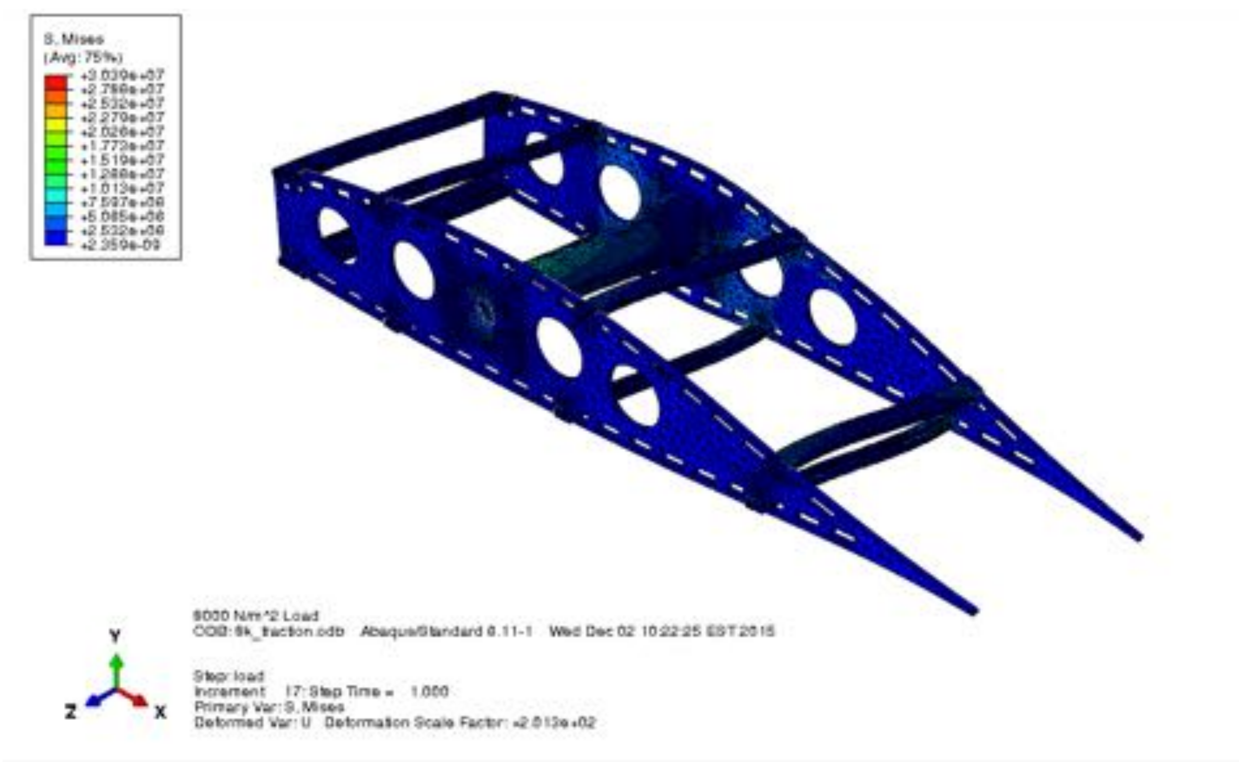

Figure 15 Vertical Displacement

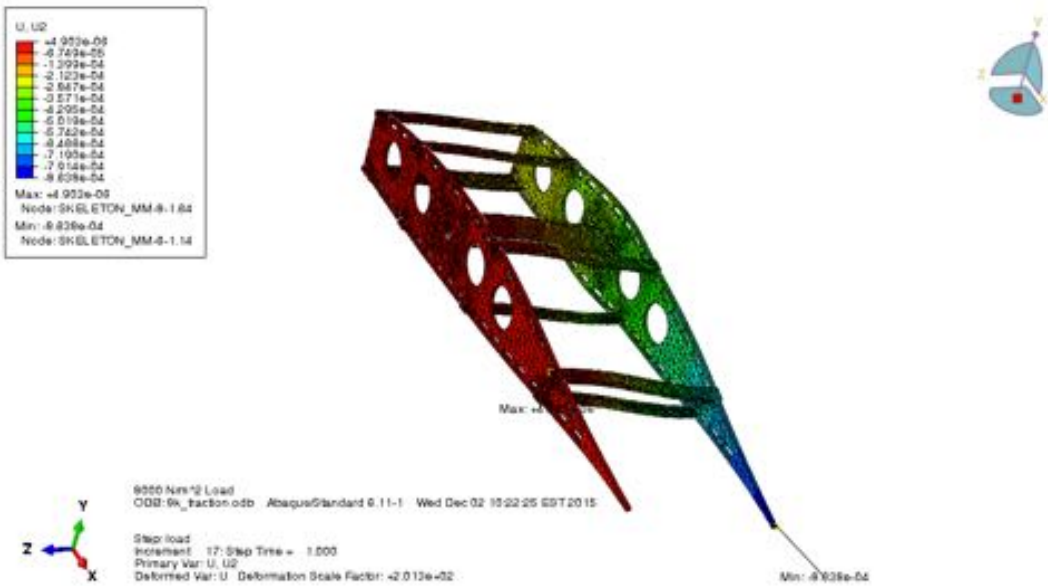

The red sections represent very little displacement while the darkest blue indicates that large displacement occurred during loading. The maximum displacement that occurred during loading was -0.9638 mm. This is a very small number but is still significant in aerospace design where the slightest movement may cause significant problems.

We decided it would be appropriate to focus the stress analysis on the Mount Tube since the majority of the stress was carried on this support. Figure 16 shows a closer look at the top surface of the tube where the higher stresses occurred.

Figure 16 Mount Tube Strees Distribution

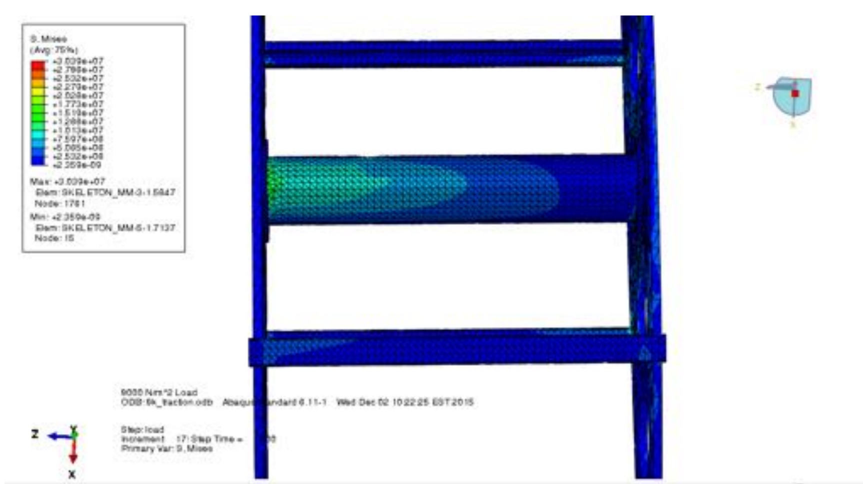

With a more indepth view of the Mount Tube stress distribution and knowing the location of the highest values of stress in the Mount Tube, we decided to generate graph sets to demonstrate how the stress changed over the loading time period. The first graph, seen in Figure 17 shows how the stress in the centroid of an element located close to the fixed panel changed over the loading time. It can be seen that the stress increased linearly with time until a maximum value of about 12 MPa was reached.

Figure 17 Centroid stress for and element near Mount Tube Base

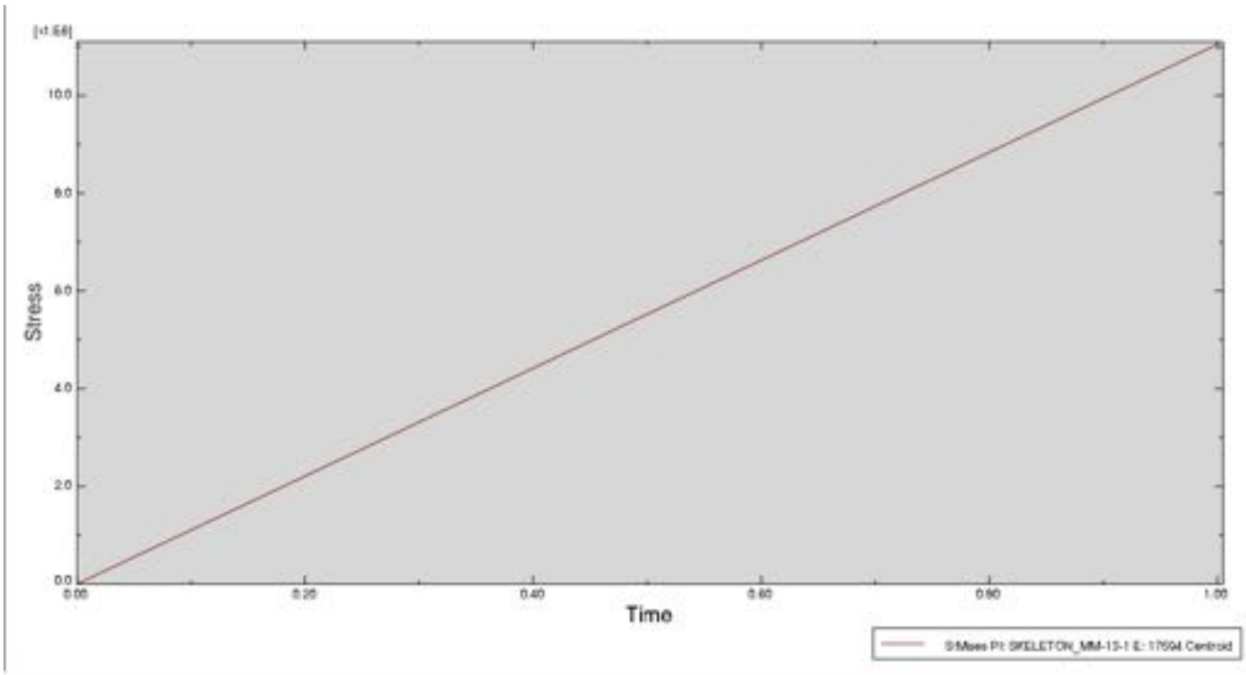

Another method used to visualize how the stress of an element changed over the loading time was to plot the values obtained at the integration points of the element, also known as the Gauss points. These are the points where the stresses obtained from the nodal values of the element are transferred to the Gauss points using the elements shape functions. Figure 18 shows how the four Gauss points of a tetrahedral element change over the loading time.

Figure 18 Gauss point stress change over time

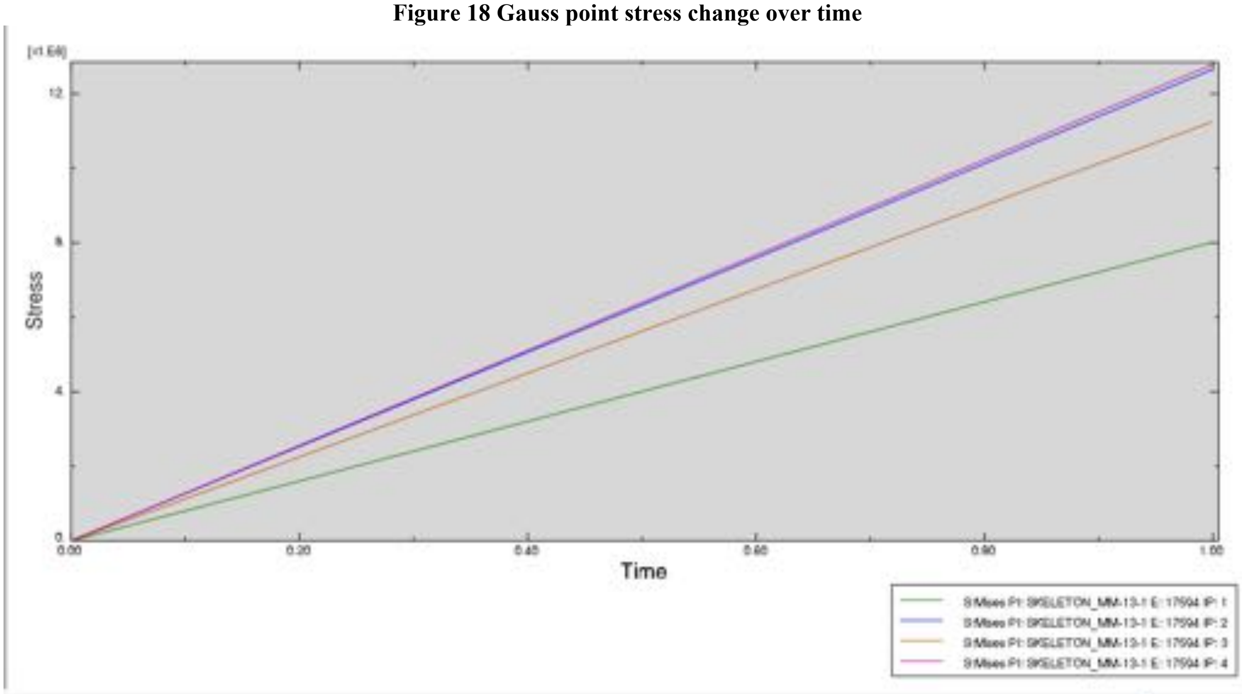

It is important to note that the values for each Gauss point are not the same for each point, or the value associated with the centroid. An average of the Gauss point stress values determines the value of the stress associated with that elements centroid. The last values that were examined were the strain values of the base of the Mount Tube. The strain in all three directions can be seen in Figure 19. These values were obtained for the centroid of the element. The strain in the x, y, and z directions can be seen as the green, yellow, and red lines respectively. The maximum strain occured in the z direction and was 0.15E-3 m/m. This makes sense because the applied surface traction is stretching the top surface of the mount tube in tension and this would cause the largest strain value to occur in the axial direction.

Figure 19 Element Strain at the Mount Tube Base

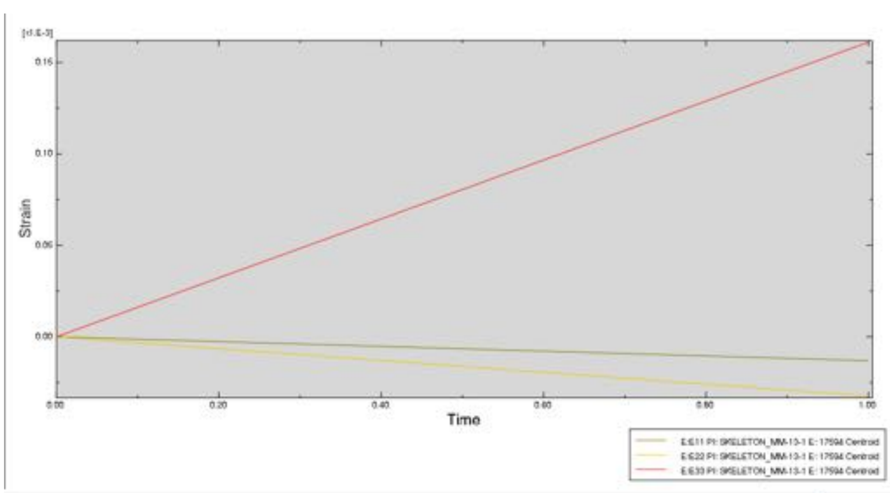

Along with examining the stress of a single element at the base of the mount tube, the stress along two paths was also examined. The first of these two paths, seen in Figure 20 is around the stress concentration in the Mount Tube. A spike in Von Mises stress can be seen at the center of the stress concentration. The second path, seen in Figure 21, which was examined, was around the circumference of the Mount Tube base. The stress in the z direction was examined to portray how the stress changes from tension on the top surface and compression on the bottom surface.

Figure 20: Von Mises stress around Mount Tube Stress Concentration

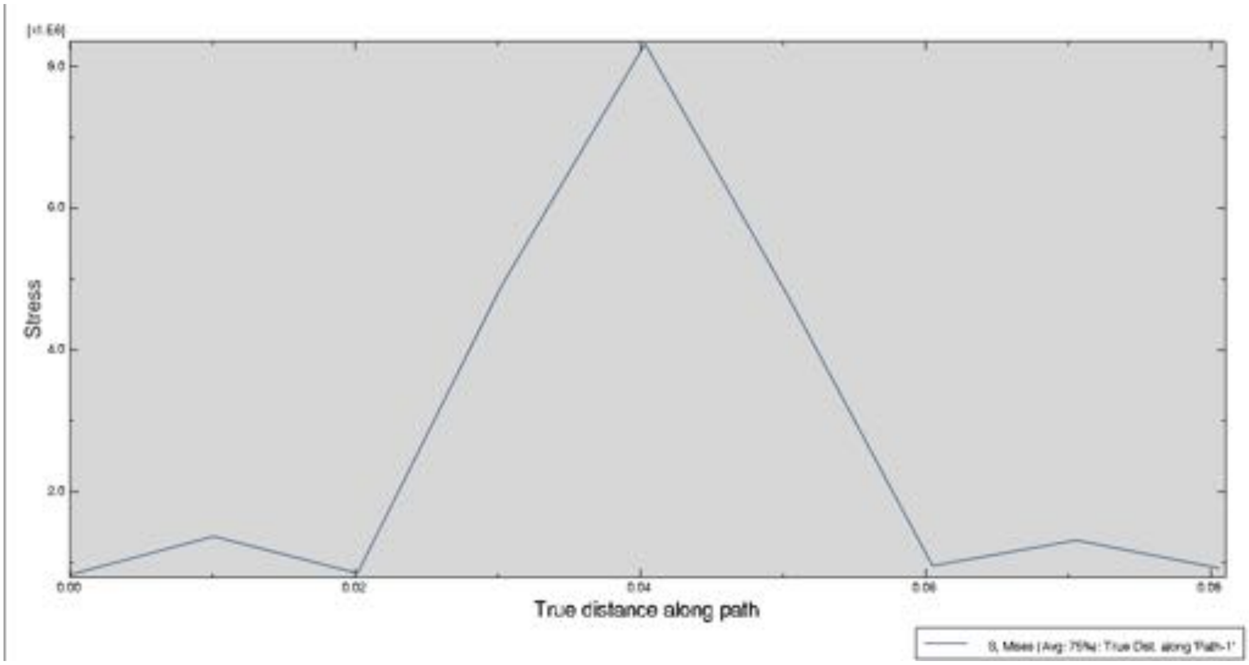

Figure 21: Stress around the circumfrence of the Mount Tube base

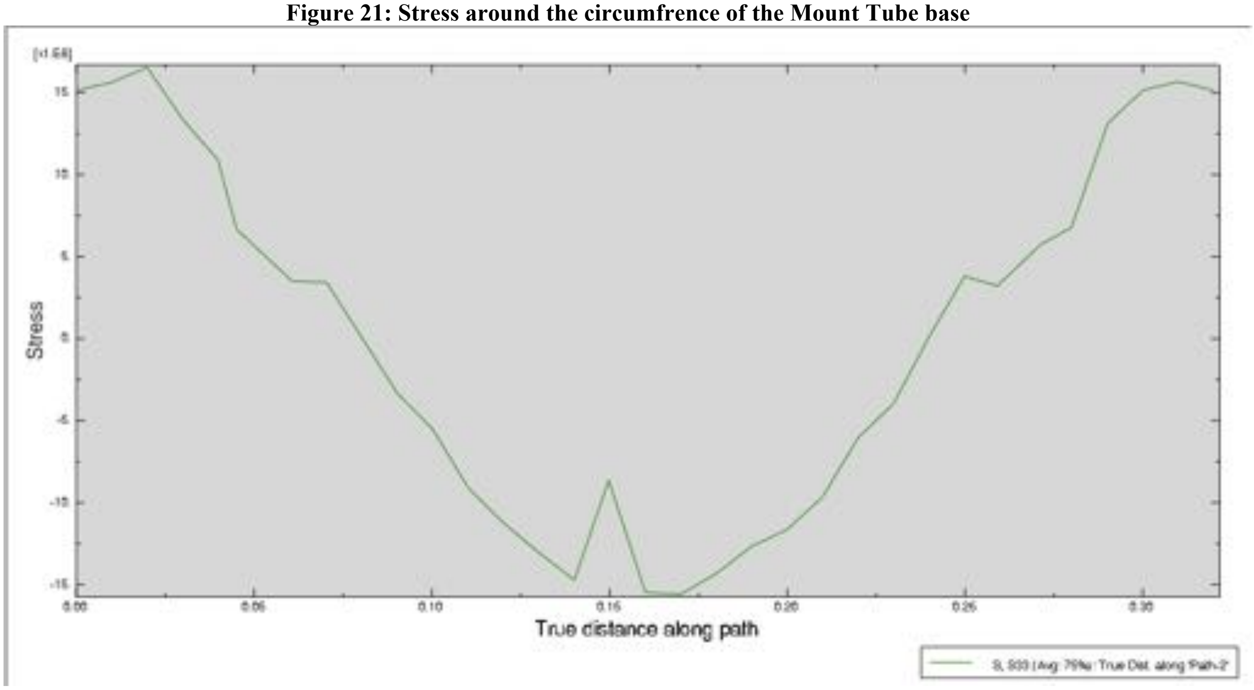

With all of the necessary results determined, final considerations were made. Determining the safety factor of the Mount Tube was the first to be considered. With a maximum Von Mises stress of 12 MPa and a yield-strength of 6061-T6 Aluminum being 310 MPa, The safety factor can be determined to be close to 26. This means that the Mount Tube is much stronger than it needs to be and will be sufficiently safe during normal operating conditions of the airfoil section. Even with the highest stress occurring in one of the smaller supports being about 30 MPa, which yields a safety factor of 10, the airfoil design is still sufficiently safe. It is still safe to assume that the main support comes from the Mount Tube and if any of the smaller supports fail the airfoil is still safe to operate if failure due to stress was the only concern.

Along with a stress analysis, a modal analysis was performed to determine the first three natural frequencies of the arfoil assembly. These Frequencies were determined to be (in cycle/time) 78.24, 88.35, and 102.41.

Failure could also occur due to large displacements. As mentioned earlier, small displacements may cause larger problems in the airfoil. This was not a design consideration that was approached in this analysis but is something to consider for future analysis. Future analysis may also include a fatigue analysis since airfoils are cyclically loaded. This was beyond the scope of this analysis but could also be a starting point for future research or experimentation.

In conclusion it was determined that the airfoil section is safe to operate under operating conditions of 300 mph and may be tested in the wind tunnel by Guidedwave. However these results do not represent a true airfoil due to the material properties that were applied, but this analysis provides an appropriate base analysis and experimentation for the project conducted by Guidedwave.

Section 8: Works Cited

ASM Material Data Sheet. ASM Aerospace Specification Metals Inc., n.d. Web. 23 Nov. 2015.

Appendix 1: Engineering Print of Airfoil Section (English Units)

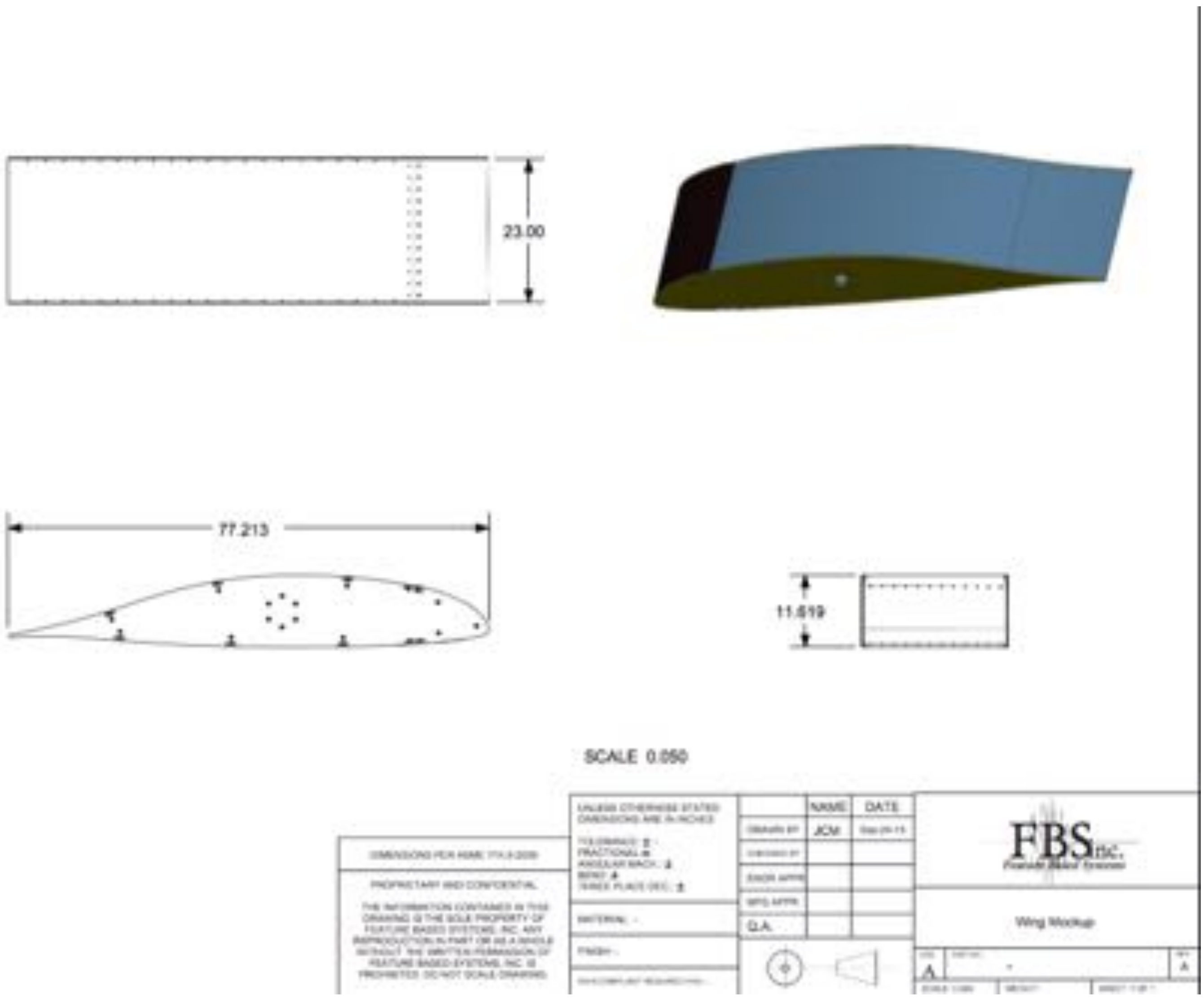

Appendix 2: Internal Shematic